

PRACTICAL EXPERIENCES IN AFM DIAGNOSTICS OF SELECTED NON-FERROUS METAL ALLOY

Vladimir Áč, Jozef Kasala, Erika Hujová, Mária Ličková

Alexander Dubcek University of Trencin, Faculty of Special Technology

E-mail: vladimir.ac@tnuni.sk

Received 9 May 2016; accepted 15 May 2016

1. Introduction

Atomic force microscope (AFM) is currently one of the most important instruments for research of material's micro-structure. Two basic contact and tapping modes are used in AFM operation. Tapping (non-contact) mode with their various alternatives overcome many of the drawbacks of the original contact-mode imaging. In tapping operation mode, the cantilever with a sharp tip (probe) is forced sinusoidally for inducing a periodic oscillation of the cantilever and the tip is by electronic control system positioned so that vibrations of the tip are in vicinity the measured sample surface [1-3]. Interactions of the sample surface atoms with the tip modify its oscillations. The oscillations are recorded and evaluated from various points of view, such as the change in oscillation amplitude (amplitude retrace), phase shift (phase retrace) between the driving signal and mechanical vibrations of the tip, height profile (height retrace) and also the non-linearity of tip oscillations. The interaction between the tip and the sample surface is highly nonlinear, because the tip moves over a long range of tip-sample potential [4,5]. The effect can be also a chaotic oscillation depending on the process parameter setting. The beneficial results of the tapping mode measurements are the phase and attenuation amplitude images which one we can obtain information about the surface components distribution of multi-component materials. Time-varying interaction forces between the vibrating tip and the sample contain detailed information about the elastic, adhesive, and dissipative response of the sample. The phase images correlate to the distribution of surface stiffness (Young's modulus) of the material [2, 5, 6]. AFM can be used to reveal subatomic structures. High spatial resolution imaging of material properties is an important task for the development of nanomaterials [7, 8].

In this contribution, we describe the practical experience with AFM measurements on Asylum Research MFP-3D Infinity equipment. We have focused on the analysis of the measurement results and their correct interpretation. The measurement was carried out on samples of non-ferrous alloys such as brass (Cu70Zn30), beryllium bronze (CuBe) and high temperature alloy CuCrZr. Non-ferrous alloys choice was deliberate, because they have very complicated structure with a number of phases and precipitation units. The goal was to achieve reproducible results in a non-contacting tapping AC mode of AFM. We watched the scattering of measured values caused by setting the detector level reference, the amplitude of the cantilever driving signal and speed of the measurement. We have also analyzed the conditions under which comes to atypical results caused by uncontrolled interference of the tip with the sample surface atoms. As a part of this work is also the analysis of how to achieve the level of monitoring of individual atoms. The obtained experimental data of our work are very extensive and therefore in this paper we use only data measured on the CuCrZr alloy. The information referred in this contribution are not exhaustive, with other above mentioned alloys were also observed another phenomenons, that will be subject to the following articles.

2. Experimental results

Experiments were carried out on the device Asylum Research MFP-3D Infinity using basic functional modes "Contact mode" and "AC air mode". The extent of this contribution is limited, so that only detailed results obtained on the sample CuCrZr alloy are here presented. The sample was prepared prior to measurement by standard metallographic technique, mechanical cutting and polishing by diamond emulsion. The aim of the experiments, it was to obtain as much data to characterize the internal structure and the resulting mechanical properties of the material.

The CuCrZr alloy has a high temperature resistance against softening (400 °C), good electrical conductivity and high hardness (170 HV). It is a material for spot welding electrodes. Its typical composition is Cu, 0.5-1 wt.% Cr and 0.04-0.15 wt.% Zr. More information about this alloy we can found for example in [9, 10].

The measurement starts with the selection of an optimal location by the integrated optical microscope of AFM equipment. The positioning accuracy of this way is at the level of several tens microns, and therefore for first, it is necessary to make surveillance AFM image with a larger dimension for exact orientation on the sample surface. In our case it is the image the surface topography (obtained in contact mode) of a sample area of 20 x 20 microns seen in Fig.1. 3D surface topography of the same area is shown in Fig. 2. In the images, we can see the groove depth exceeding 100 nm, invisible by the naked eye, which means that polishing was insufficient. For further measurements, there was selected the area of 5 x 5 microns with small vertical profile (this area is marked by a square in Fig.1).

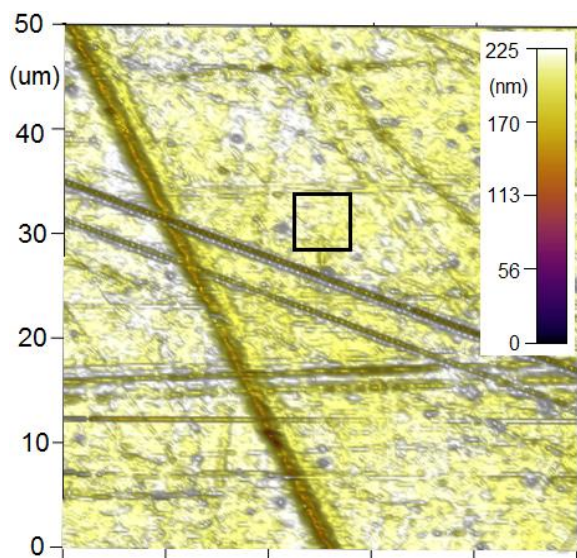


Fig. 1: Surface image of CuCrZr sample in contact mode (size 20 x 20 μm^2),

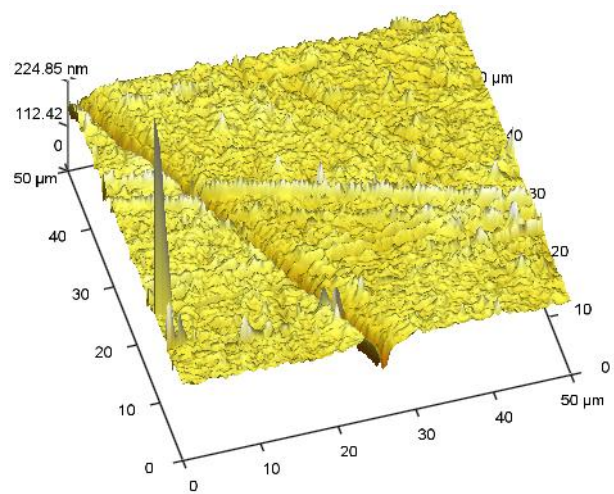


Fig. 2: 3D image of CuCrZr sample in contact mode (size 20 x 20 μm^2), the same area as in Fig. 1.

All following measurements were made in a non-contact (tapping) AC mode of AFM. In this mode, three basic parameters of the tip oscillation at the sample surface are evaluated: height profile (height retrace), attenuation of oscillation amplitude (amplitude retrace) and phase difference between the driving signal and the tip vibration (phase retrace). Fig.3 shows the result of the phase profile for the selected area (marked in Fig.1) of the specimen and Fig. 4 is its 3D image in amplitude characteristics.

More information is shown in Fig.5. from other detail (1 square μm) of the height profile from area marked in Fig.3. Fig. 6 shows the 3D image of the phase characteristics of the same detail as seen in Fig.5. In this figure, a massive phase response of local surface areas

is shown. The phase deviation has both positive and negative direction, suggesting a large variation of the force fields on sample surface.

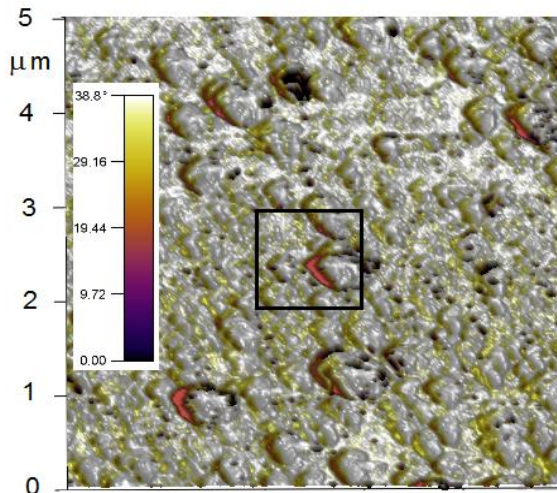


Fig. 3: Detail (size $5 \times 5 \mu\text{m}^2$) of surface image of CuCrZr sample in AC mode and phase characteristics.

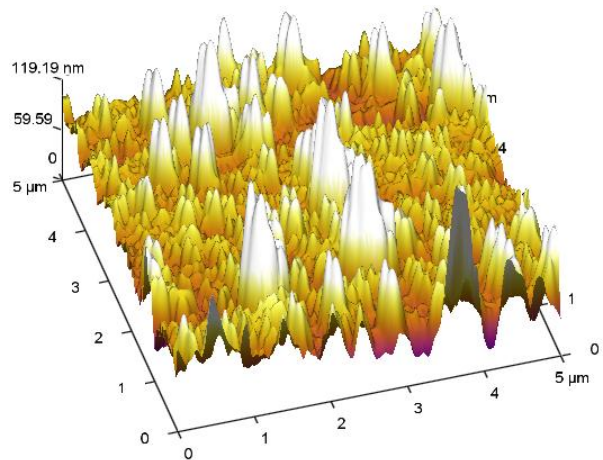


Fig. 4: 3D image of surface CuCrZr sample in AC mode (amplitude characteristics from the same area as in Fig. 3.)

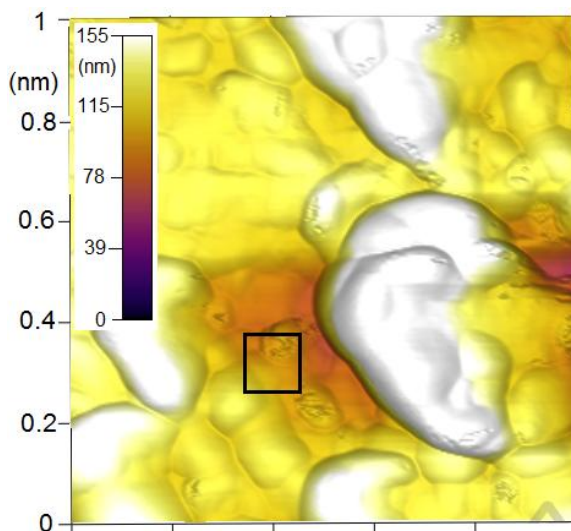


Fig. 5: Detail $1 \times 1 \mu\text{m}^2$ marked by a square in Fig.3.(height retrace).

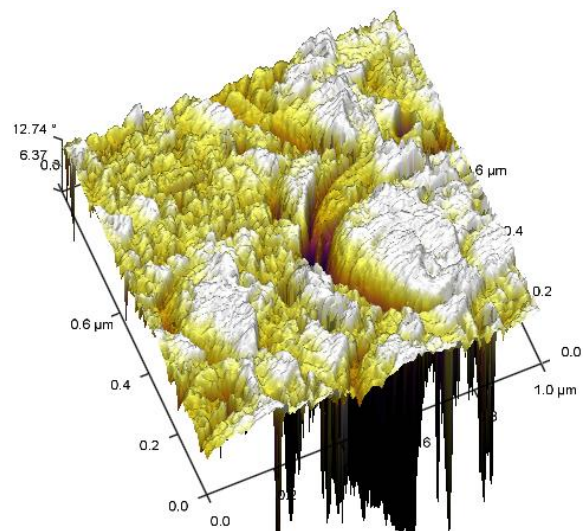


Fig. 6: 3D image of phase characteristics (the same area as in Fig. 5.)

The following step of structural analysis was concentrated to see the surface at sub nanometer distance. In Fig.7 we can see a detailed image of the amplitude characteristics of the area $128 \times 128 \text{ nm}^2$ (square area marked in Fig.5). Dark points in Fig.7 represent the individual atoms. It should be noted that any dark spot in Fig.7 (a lower amplitude of tip oscillations) is accompanied by reflective paler point located to the right (with less depression of the tip oscillation and its higher amplitude). This effect may be deemed to be systemically equipment measurement error caused by the tip control algorithm at strong interaction of the tip with the sample surface. This is confirmed by comparison of pair images seen in Fig.9 and Fig.10, showing the difference in measurement results. The measurement time of one line in Fig. 9 was 5 seconds in comparison with 1 second of the one line measurement in Fig.7. The distance of reflex spots to black spots is 3 times smaller in size at slower measurement speed.

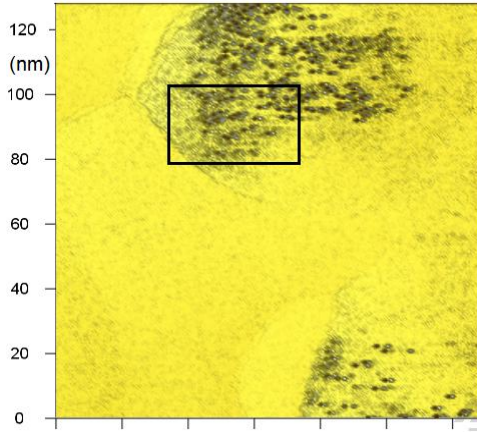


Fig. 7: Detail $128 \times 128 \text{ nm}^2$ marked by square in Fig.5.(amplitude retrace).

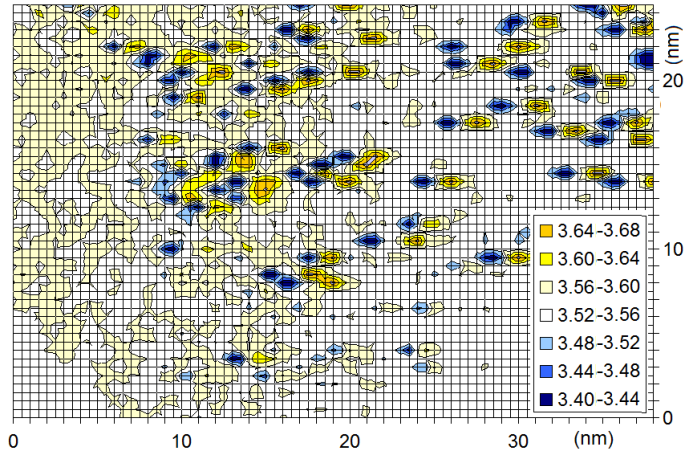


Fig. 8: Reconstruction of the deployment of individual atoms on area marked in Fig. 7. ($f = 1 \text{ Hz}$)

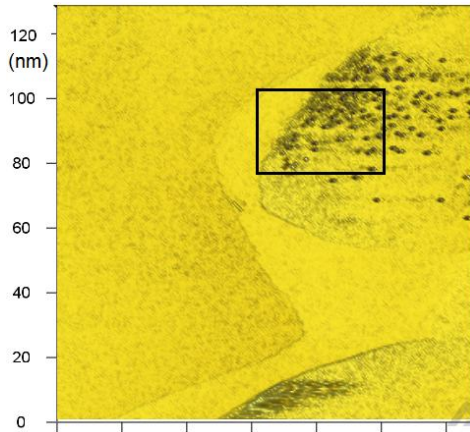


Fig. 9 Other detail $128 \times 128 \text{ nm}^2$, (amplitude retrace) at line frequency $f=0.2 \text{ Hz}$.

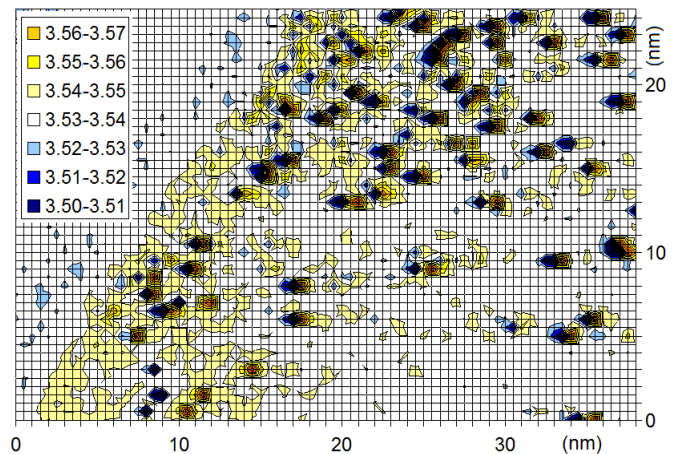


Fig. 10: Reconstruction of the deployment of individual atoms on area marked in Fig.9 (line frequency $f = 0.2 \text{ Hz}$)

3. Discussion and conclusion

The measurement results presented here show that the AFM brings new insights into the material structure. In comparison to others diagnostics (e.g. Scanning Electron Microscopy), the AFM technology has the advantage to investigate the structure on the atomic level without special claims. The problem lies in finding the right interpretation of measurement results. This needs to be based on the known information published in scientific literature and use them at analysis of AFM measured results. The CuCrZr alloy precipitates at some preparing conditions have a bimodal distribution of precipitate size. The coarse precipitates are pure Cr and Cu₅Zr, the dispersed fine precipitate is CrCu₂(Zr,Mg) and pure Cr ranging from 1 to 50 nm. The coarse phases formed during solidification and were left undissolved during solid solution. The fine precipitates are the hardening precipitates that form due to decomposition of the supersaturated solid solution during aging [9, 10].

Let us apply the above knowledge to interpret the results on our measurements. Three types of structural units are seen in Fig.3. Larger details in Fig.3 and Fig.4 have the typical dimension of about 500 nm and they have a significantly higher response in amplitude characteristics due to less attenuation of the tip vibration. Among them there are smaller areas with less amplitude (greater damping of tip vibration) and dimension of approximately 200 nm and finally else smaller units with dimension approx. 100 nm and less. These are very good

seen in Fig.3 as a dark small spots. These units have very large phase response and that could be Cr precipitates. Compound Cu_5Zr or CrCu_2 should be formed to larger formations, because the material with lighter atoms, or lower density causes less depression of tip vibration and the contrary.

We close the inspirational example by the statistical frequency distribution of amplitude response levels for the case shown in Fig. 11. The arrowed local maxima (1-7) could be attributed to the individual components of the structure of the studied sample. Fig. 11 shows the symmetrical arrangement of local maxima around the absolute maximum resulting from the reflection effects. The exception is a maximum marked by arrow 7. It has greater amplitude and may to indicate for example structural defects, which have zero interaction with oscillating AFM tip. This consideration requires more thorough investigation. As a result, this view could lead to the possibility of a kind of spectral analysis of the atomic structure of the material surface.

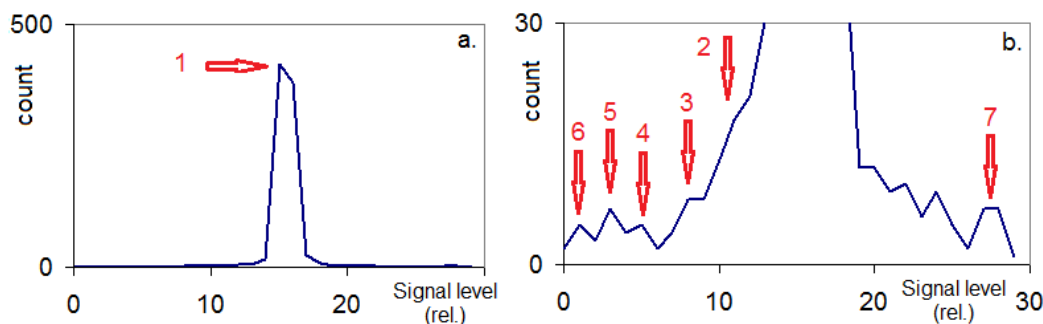


Fig. 11: Frequency of amplitude level distribution for image in Fig. 10.

Acknowledgement

The authors would like to thank Assoc. Prof. Rudolf Pernis, PhD. for useful consultations. This work was supported by internal grant of Faculty of special technology TnUAD.

4. References

- [1] S. Misra, H. Dankowicz and M.R. Paul: *Proc. of The Royal Society A* (2008), online: <http://rspa.royalsocietypublishing.org/content/464/2096/2113>
- [2] S.N. Magonov, V. Elings, M.H. Whangbo: *Surface Science* **375** (1997), L385-L391
- [3] A.F. Sarioglu and O. Solgaard: *Ch 1 in Scanning Probe Microscopy in Nanoscience and Nanotechnology 2*, B. Bhushan (Ed.), Springer 2011, XXVI, ISBN:978-3-642-10496-1, pp.3-37
- [4] G. Couturier, R. Boisgard, L. Nony, and J. P. Aime: *Rev. Sci. Instrum.* **74** (5), 2726-2734 (2003)
- [5] L. Yuan, Q. Jian-Qiang, and L. Ying-Zi: *Chin. Phys. B Vol. 19, No. 5* (2010) 050701-6 online: <http://cpb.iphy.ac.cn/fileup/PDF/2010-050701-32.pdf>
- [6] O. Sahin and N. Erina: *IOP Publ., Nanotechnology* **19** (2008) 445717 (9pp)
- [7] L. Gross, F. Mohn, N. Moll, P. Liljeroth, G. Meyer: *Science* 29 Aug 2009, Vol **325**, p. 1110-3, DOI: 10.1126/science.1176210
- [8] M. Emmrich, F. Huber, F. Pielmeier, at all: *Science* 17 Apr 2015, Vol.**348**, Issue 6232, pp. 308-311, DOI: 10.1126/science.aaa5329
- [9] Z. Mei, L. Guobiao, W. Zidong, Z. Maokui: Analysis of precipitation in a Cu–Cr–Zr Alloy, *China Foundry Research & Development* Vol.5 No.4, pp. 268-271
- [10] P-E Frayssines, J-M Gentzittel, A Guilloud, et al., *The Royal Swedish Academy of Sciences Physica Scripta*, Volume **2014**, Number T159